STAT1-Regulated Lung MDSC-like Cells Produce IL-10 and Efferocytose Apoptotic Neutrophils With Relevance In Resolution of Bacterial Pneumonia

Stephanie L. Poe[1,2], **Meenakshi Arora**[1], **Timothy B. Oriss**[1], **Manohar Yarlagadda**[1], **Kumiko Isse**[3], **Anupriya Khare**[1], **David E. Levy**[4], **Janet S. Lee**[1], **Rama Mallampalli**[1], **Anuradha Ray**[1,2], and **Prabir Ray**[1,2]

[1]Division of Pulmonary, Allergy, and Critical Care Medicine, Department of Medicine, University of Pittsburgh School of Medicine, Pittsburgh, PA 15213

[2]Department of Immunology, University of Pittsburgh School of Medicine, Pittsburgh, PA 15213

[3]Department of Pathology, University of Pittsburgh School of Medicine, Pittsburgh, PA 15213

[4]Departments of Pathology and Microbiology, New York University, New York, New York 10016

Abstract

Bacterial pneumonia remains a significant burden worldwide. Although an inflammatory response in the lung is required to fight the causative agent, persistent tissue-resident neutrophils in non-resolving pneumonia can induce collateral tissue damage and precipitate acute lung injury. However, little is known about mechanisms orchestrated in the lung tissue that remove apoptotic neutrophils to restore tissue homeostasis. In mice infected with *Klebsiella pneumoniae*, a bacterium commonly associated with hospital-acquired pneumonia, we show that interleukin-10 is essential for resolution of lung inflammation and recovery of mice after infection. Although IL-10–/– mice cleared bacteria, they displayed increased morbidity with progressive weight loss and persistent lung inflammation in the later phase after infection. A source of tissue IL-10 was found to be resident CD11b$^+$Gr1^{int}F4/80$^+$ cells resembling myeloid-derived suppressor cells that appeared with a delayed kinetics after infection. These cells efficiently efferocytosed apoptotic neutrophils, which was aided by IL-10. The lung neutrophil burden was attenuated in infected STAT1–/– mice with concomitant increase in the frequency of the MDSC-like cells and lung IL-10 levels. Thus, inhibiting STAT1 in combination with antibiotics may be a novel therapeutic strategy to address inefficient resolution of bacterial pneumonia.

Introduction

Bacterial infection leading to pneumonia is a leading cause of morbidity and mortality worldwide with more than 3 million cases occurring annually in the United States alone and

Correspondence should be addressed to: Prabir Ray PhD. or Anuradha Ray, Ph.D., Department of Medicine, Pulmonary, Allergy and Critical Care Medicine, University of Pittsburgh School of Medicine, 3459 Fifth Avenue, MUH A628 NW, Pittsburgh, PA 15213, Telephone: (412) 802-3192(1), Fax: (412) 692-2260, rayp@pitt.edu (P.R.) or raya@pitt.edu (A.R.).

resulting in 40,000 to 70,000 deaths each year [1]. Additionally, the majority of deaths during the 1918–19 influenza pandemic were actually due to secondary bacterial infections following viral clearance [2]. Characteristically, defense against pathogenic bacteria involves a set of finely tuned orchestrated events whose goal is to rapidly mount an innate immune response to clear the pathogen [3,4]. The cells of the innate immune response that are able to phagocytose and kill the internalized bacteria are the alveolar macrophages and neutrophils [3,4]. However, depending on the nature of the pathogen and the cells involved in bacterial clearance-macrophages versus neutrophils, the cytokine environment may modulate the outcome of bacterial clearance [5].

Typically, alveolar macrophages (AMs) participate initially and their numbers dwindle as neutrophils are rapidly recruited to the site of infection [6]. Neutrophils produce a range of products including reactive oxygen species and proteases that are not only harmful for the pathogen but also for the host's own cells [1,7–10]. Therefore, once the pathogen is cleared, it is crucial for the host to mount an appropriate anti-inflammatory response to limit further neutrophil recruitment and clear the dead cells. However, bystander tissue injury caused by unmitigated inflammation after infection can initiate and lead to the progression of acute lung injury (ALI) that can be fatal. Indeed, severe pneumonia is a common underlying cause of acute lung injury and its more formidable form, acute respiratory distress syndrome (ARDS) [1,11]. It is, therefore, important to understand the molecular and cellular mechanisms that mediate innate immune system dysfunction so that tissue homeostasis after infection can be rapidly restored with therapeutic intervention, if necessary.

Excess tissue IL-10 levels early after infection inhibits bacterial clearance thereby acting as a negative regulator of host defense [4,12,13]. However, IL-10 is also known to be important for maintenance of homeostasis as well as regulation of neutrophil clearance (decrease survival/efferocytosis) [4,13–16]. These two observations, while seemingly contradictory, point to the need for early absence of IL-10 to facilitate bacterial clearance but its presence being necessary during the resolution phase of an immune response. A central unanswered question in the context of bacterial pneumonia is which cell type(s), with the potential to produce IL-10 in the lung tissue, like AMs in the alveolar lumen, aid in the removal of apoptotic neutrophils (efferocytosis) effecting resolution of inflammation. This question is important because neutrophils in the alveolar space represent only a fraction of the extravasated neutrophils in the inflamed lung and do not necessarily track with parenchymal neutrophil burden [17,18]. In contrast, interstitial neutrophils have been found to be more intimately associated with clinically relevant measures of ALI, such as increased microvascular permeability and decreased lung compliance [7,8,10]. Thus, there appears to be an indispensible role for additional cellular players in the alveolar interstitium to limit lung injury by inhibiting the continuous tissue influx of neutrophils after infection and to efferocytose apoptotic neutrophils.

We recently described a CD11b$^+$Gr1^{int}F4/80$^+$ regulatory cell population in the lung that expands in response to LPS exposure in a TLR4/MyD88-dependent manner [19]. We showed that these cells have the ability to suppress Th2 effector responses via secretion of IL-10. These cells also secrete IL-6 and GM-CSF, but low levels of IL-12. Due to their close resemblance to myeloid-derived suppressor cells (MDSCs), these Gr1^{int} (Ly6G^{int}Ly6C^{lo})

cells are now recognized as lung MDSCs with resemblance to PMN MDSCs [20]. In a recent study of lung infection with influenza virus A, absence of TLR7 promoted a monocytic MDSC population that promoted Th2 responses [21]. Thus, it appears that the nature of the insulting agent together with the type of the induced MDSC and the mediators produced by it collectively influence the T helper response.

It is known that mice lacking functional MyD88 signaling have increased susceptibility to a number of infectious pathogens, including the Gram negative bacterium *Klebsiella pneumoniae* [22]. *K. pneumoniae* is a common bacterial species acquired by nosocomial infections that can cause pneumonia in severely ill patients with a high rate of morbidity and mortality. In fact, *K. pneumoniae* was found to be the third most commonly isolated organism from intensive care units in the US [23]. In our previous study, we observed IL-10 production by tissue-resident MDSC-like cells in response to LPS [19]. In this study we addressed whether these cells represent a source of IL-10 after infection with *K. pneumoniae* and if so, whether this is beneficial for the host. This question arose because presence of IL-10 early after infection with *K. pneumoniae* was deleterious and increased bacterial load in the lung. However, IL-10 was crucial for resolution of inflammation and eventual recovery of mice late after infection. The MDSC-like cells were found to expand in the lungs with delayed kinetics in response to bacterial infection and therefore produced IL-10 only in the later phase of infection. Functionally, the cells efferocytosed apoptotic neutrophils that was partially dependent on IL-10. In our efforts to identify mechanisms that would increase the MDSC: neutrophil ratio that would help the resolution process, we found that deletion of STAT1 caused a doubling of MDSC-like cells with concomitant reduction of tissue neutrophils. In the absence of STAT1 signaling, IL-6 and IL-10 levels in the lung increased, both of which signal through STAT3, a known mediator of proliferation and survival of MDSC-like cells [20,24].

Results

Early Versus Late Interleukin 10 during infection By *Klebsiella Pneumoniae*

IL-10 has been negatively associated with the deployment of rapid defense mechanisms against bacterial infection [4,12,13]. However, its role in the resolution of tissue inflammation induced to clear the pathogen has not been adequately addressed. Our goal was to determine whether wild-type (WT) and IL-10–/– mice differentially respond to acute bacterial infection over time. To address this goal, we wished to use a dose of the bacterium that would allow ~50% of the wild-type (WT) mice to recover from infection and observe whether lack of IL-10 would make a difference in this recovery. Towards this end, we infected WT C57BL/6 mice with 100 or 1000 colony forming units (CFU) of *K. pneumoniae*. All mice infected with the lower dose of 100 CFU reproducibly recovered from bacterial infection without any morbidity or mortality. With the higher dose of 1000 CFU, however, at 72 h after infection, ~ 50% of the WT mice displayed continued loss of weight and body temperature, greater systemic dissemination of bacteria, (Supplementary Figure 1, panels a–c) and appeared huddled and withdrawn from food. These moribund mice were placed in one group while the remaining 50% that received the same high bacterial dose, but did not appear sick and were active, were labeled survivors and placed in the other

group. The level of IL-10 was significantly higher in the lungs of the sicker mice and correspondingly, the percentage of polymorphonuclear neutrophils (PMNs), required for rapid bacterial clearance, was lower in the lungs of this group (Supplementary Figure 1, panels d and e). Thus a dose of 1000 CFU was chosen to examine whether presence or absence of IL-10 made any difference to the recovery of mice after bacterial infection.

To assess the role of IL-10 in defense against *K. pneumoniae*, WT and IL-10–/– mice were infected with 1000 CFU of the bacterium. We compared the outcome in the two groups with respect to inflammation, bacterial burden in the lung, systemic bacterial load and weight loss. Early after infection at 48 h, the IL-10–/– mice showed limited lung pathology and carried lower bacterial burden in the lung compared to the WT mice (Figure 1a). These results were in line with previous observations of delayed mortality and reduced bacterial burden in the lungs of mice in which IL-10 was neutralized prior to infection with a dose of *K. pneumoniae* that was lethal for the strain of mouse used (CD-1) [12]. The difference between the prior study and ours is that we used a dose where 50% of mice would die in order to study effects of complete IL-10 deficiency on lung health and bacterial dissemination late after infection. The rationale for our experimental design was that while lack of IL-10 initially might help in bacterial clearance, it is unknown how its absence would impact resolution of lung inflammation and recovery after infection.

The 50% of the WT mice that appeared close to death on day 3 after infection by virtue of huddled appearance, withdrawal from food and loss of body weight and temperature were euthanized. In contrast, fewer (~20%) of the IL-10–/– mice looked moribund at this time point. By 144 h, while the remaining 50% WT mice looked active and on the road to recovery, all of the IL-10–/– mice met criteria for euthanasia, which included continued loss of body weight, withdrawal from food, loss of body weight and temperature and needed to be sacrificed along with the WT survivors (which were active and appeared to have recovered) to assess various outcome measures. Analysis of lung histology using Metamorph showed that compared to the lungs of WT mice, those of IL-10–/– mice at 144 h post-infection harbored significantly greater inflammation (Figure 1b). However, we did not observe increased bacterial dissemination in the IL-10-deficient mice at 144 h (Figure 1b). Strikingly, using weight loss as a global measure of health decline, we observed that the IL-10–/– mice continued to lose weight after infection whereas the WT survivors began to regain the weight lost during the initial phase of infection with the two groups beginning to diverge at 72 h after infection (Figure 1c). Myeloperoxidase (MPO) activity (a measure of PMN infiltration) was also increased in the IL-10–/– mice 144 h post infection (Figure 1d). Upon further investigation of what criteria distinguished the WT from their IL-10–/– counterparts at 72 h, a time point at which the surviving WT and the IL-10–/– mice began to diverge with respect to weight loss, we found that the MPO activity and the PMN:Mac ratio in the BAL fluid was greater in the IL-10–/– mice as compared to that in the WT mice (Supplementary Figure S2, panels a and b). However, the majority of the IL-10–/– mice had 2 logs lower CFU in their blood at this time point compared to the WT mice (Supplementary Figure S2c). Thus, in our analysis, the key difference at 72 h that was disadvantageous to the IL-10–/– mice was more inflammation in the lungs as compared to that in the WT

counterparts. No systemic bacteria were detected in the surviving WT mice after 8 days of infection (Supplementary Figure S2d).

We examined the levels of two cytokines, IL-17A and TNF-α, and the neutrophil chemoattractant KC in the lungs of the mice 144 h after infection whose combination was found to promote lung neutrophilia in response to fungal infection in our recent study [25]. As shown in Figure 1d, the levels of all of these molecules were significantly higher in the lungs of the IL-10-deficient mice at 144 h after infection, which might explain the increased PMN burden in these mice late after infection (Figure 1 **and** Supplementary Figure S2). qRT-PCR analysis of steady-state RNA levels at 144 h for the most part also matched the protein data (Supplementary Figure S3). The lack of correspondence between RNA and protein for TNF-α may be due to posttranscriptional regulation of protein expression [26]. Taken together, these results suggested that the increased sickness observed in the IL-10−/− mice over time was not due to failure to clear bacteria but that the mice continued to harbor an overwhelming inflammatory response in the lungs in the absence of IL-10, which was already evident at 72 h after infection.

Gr1^{int} MDSC-like cells expand in response to *K. pneumoniae* and produce IL-10

Alveolar macrophages (AMs) are known to participate in the removal of cellular debris following infection. However, because they are confined to the alveolar lumen, there is a requirement for additional cellular players to remove apoptotic neutrophils in the lung interstitium to restore tissue homeostasis. Our previous work identified a myeloid cell with the phenotype CD11b$^+$Gr1^{int}F4/80$^+$ resembling myeloid-derived suppressor cells (MDSCs) whose numbers increase in the lung tissue in response to LPS in a dose-dependent fashion and which produce IL-10 [19]. As previously described [19], the cells are largely Ly6G^{int}/Ly6C$^{lo/−}$ and resemble granulocytic MDSCs. These cells constitute >60% of F4/80+ cells in the lung at 72 h after LPS instillation or bacterial infection. Given the anatomical location of these lung MDSC-like cells as well as their ability to proliferate in response to LPS, we examined the kinetics of their expansion and IL-10-producing ability in response to *K. pneumoniae*. As shown in Figure 2a, the number of the Gr1^{int} MDSC-like cells (labeled as Gr1^{int} cells) did not change at 24 h after infection but increased significantly at 72 h after infection. Since AMs are also known to produce IL-10, we next simultaneously investigated the expansion of both AMs and the Gr1^{int} cells after infection with 1000 CFU of *K. pneumoniae*. More AMs than Gr1^{int} cells were recovered from the lungs of naïve mice. At 72 h after bacterial infection, however, the profile was reversed with fewer AMs than MDSC-like cells present in the lungs of the infected mice (Figure 2a). Typically, AMs participate very early after infection and their numbers dwindle as neutrophils are rapidly recruited to the site of infection [6], which was observed by us as well (not shown). However, although the AMs reappear over time to be able to clear dying neutrophils in the alveolar lumen, at 72 h post-infection, the MDSC-like cells were clearly more abundant compared to AMs (Figure 2a). These data suggest a carefully orchestrated mechanism the host has evolved to simultaneously allow for an appropriate inflammatory response to bacterial challenge with subsequent expansion of MDSC-like Gr1^{int} cells 72 h post infection, to temper inflammation and prevent tissue damage. Importantly, although both AMs and lung Gr1^{int} cells were able to secrete IL-10, the total contribution of IL-10 from the interstitial

Gr1^{int} cells outweighed the amount of IL-10 from the AMs in the lumen late after infection (Figure 2b). We examined IL-10 production from tissue PMNs, Gr1^{int} and total F4/80+ cells isolated from the lungs of mice at 72 h after infection with 100 versus 1000 CFU of bacteria by intracellular staining techniques. As shown in Figure 2c, the frequency of IL-10-secreting cells was highest in the Gr1^{int} population with 100 CFU of infection. The frequency of IL-10-secreting Gr1^{int} cells appeared to diminish with the higher bacterial dose. The results of these experiments showed that with the passage of time after infection when bacteria and PMNs infiltrate the tissue, the Gr1^{int} cells expand as IL-10-producing cells in the lung. They appear with a delayed kinetics so as not to produce IL-10 too early to impede PMN recruitment for bacterial clearance.

Gr1[int] MDSC-like cells are outnumbered by neutrophils at high bacterial dose

While our studies and previous literature collectively show that the host deploys its armamentarium of cells in a highly regulated fashion to combat infection, the delicate balancing act of mounting inflammation to eliminate the pathogen and then later curbing it to restore homeostasis is not always successful. In patients who fail to recover from bacterial pneumonia, overwhelming tissue inflammation precipitates ALI [1,7–10]. Since a dose of 100 CFU of bacteria led to complete recovery of all mice while 1000 CFU caused 50% mortality in our study, we examined the PMN:Gr1^{int} ratio in the lungs of the mice in response to these doses 24 and 72 h after infection. Our analysis showed that the numbers of Gr1^{int} cells do not keep up with those of infiltrating neutrophils at a higher bacterial burden (Figure 3a,c). In particular, in moribund mice infected with 1000 CFU of bacteria, the ratio of PMN:Gr1^{int} cells was ~20, compared to a ratio of ~7 in mice with less weight loss (survivors) (Figure 3b) and 2–4 in mice infected with 100 CFU (Figure 3c).

Lung MDSC-like cells have the ability to efferocytose apoptotic neutrophils

Our next question in the study was about the function of the Gr1^{int} cells-whether these IL-10-secreting cells appearing with a delayed kinetics in the tissue have the ability to remove dying PMNs. The term "efferocytosis" describes the phagocytosis of apoptotic cells, a process shown to promote and require IL-10 [13,16,27]. Although AMs are known to participate in PMN clearance in the lumen, which cell types mediate a similar process in the interstitium is poorly understood. In order to investigate whether the IL-10-producing lung Gr1^{int} cells have efferocytic potential, we labeled both apoptotic PMNs and lung Gr1^{int} cells. The labeled cells were incubated together in culture medium and uptake of the fluorescently labeled PMNs by the Gr1^{int} cells was examined. Flow cytometric analysis suggested the ability of the Gr1^{int} cells to efferocytose apoptotic PMNs (Figure 4a) which was further substantiated by confocal imaging methods (Figure 4b). Z-stack projections confirmed that the neutrophils were contained within the Gr1^{int} cells (not shown). Furthermore, neutralization of IL-10 by anti-IL-10 in the efferocytosis assay dose-dependently reduced the efferocytic efficiency of the Gr1^{int} cells (Figure 4c). Thus, IL-10-producing lung Gr1^{int} cells show the capacity to ingest apoptotic neutrophils and IL-10 enhances the efferocytic potential of these Gr1^{int} cells.

Regulation of Gr1^{int}:PMN ratio by STAT1

Our data showing efferocytic potential of the Gr1^{int} cells (Figure 4) and blunting of their numbers compared to PMNs with high bacterial burden (Figure 3) led us to then ask what mechanisms limit Gr1^{int} cellular expansion in the interstitium since if their numbers could be expanded, their regulatory properties could be better harnessed to limit immune-mediated pathology.

Tumor-associated MDSCs have been shown to be dependent on STAT3 for both expansion and mediator production [20]. In fact, a recent publication highlights the importance of STAT3 signaling downstream of Hsp72/TLR2 via autocrine IL-6 for MDSC suppressive function [28]. In our experiments, neutralization of IL-6 blunted Gr1^{int} numbers in *ex vivo* cultures of the cells (Supplementary Figure S4c). STAT1 and STAT3 are known to counterbalance each other with effects on both cytokine production and cellular plasticity [20,24,29–31]. Given our interest in expanding the Gr1^{int} MDSC-like cell type in the lung towards clearance of apoptotic PMNs, we asked whether deletion of STAT1 signaling would help promote Gr1^{int} cells and lower PMNs in defense against *K. pneumoniae*. Towards this end, WT and STAT1−/− mice were infected with 1000 CFU of bacteria. At 72 h post infection, the STAT1−/− mice survived and showed clearer lungs by histological examination compared to the WT mice (Figure 5a). Since STAT1, downnstream of type I and II IFNs controls activation of phagocytic cells for pathogen killing [32], bacterial dissemination was significantly higher in the STAT1-deficient mice (Supplementary Figure S5a). However, it is possible that the mice did not immediately succumb to infection because STAT1 deficiency was somewhat compensated by adequate levels of TNF-α (Supplementary Figure S5b), which is also important for phagocyte activation [33]. Most importantly, the reduced lung histopathology may have also sustained the mice. With regard to effects on the myeloid cells, the STAT1−/− mice showed almost a doubling in the numbers of Gr1^{int} cells in the lung with significant reduction in PMN numbers as compared to the WT mice (Figure 5b). The lower numbers of PMNs in the STAT1−/− mice also correlated with reduced MPO activity in the BAL fluid (Figure 5c). The tissue IL-10 level as well as IL-10 gene expression in the Gr1^{int} cells was greater in the STAT1−/− mice (Figure 5, **panels d and e**). The efferocytic potential of the STAT1-deficient Gr1^{int} cells was found to be largely intact (Figure 5f). This is important since STAT1 controls the expression of selected molecules involved in phagocytosis [34]. Since the IL-6/STAT3 axis promotes proliferation of MDSCs, we were curious to determine whether the IL-6 level in the lungs of the STAT1−/− mice was increased as compared to that in WT mice which was found to be true (Figure 5g). Because the level of IL-6 was higher in the lungs of STAT1−/− mice, we asked whether STAT3 signaling was enhanced in Gr1^{int} cells isolated from these mice. In these experiments, LPS was used as a surrogate for *K. pneumoniae* since treatment of STAT1−/− mice with LPS also resulted in increased frequency of the MDSC-like cells (not shown). As shown in Figure 5h, IL-6 efficiently induced STAT3 phosphorylation in MDSC-like cells harvested from naïve WT (shown) or STAT1−/− mice. When cells were isolated from LPS-treated WT and STAT1−/− mice, higher pSTAT3 levels were detected in response to IL-6 in the STAT1-deficient Gr1^{int} cells (Figure 5h). Thus, the increased IL-6 levels in the lungs of STAT1−/− mice (Figure 5g) combined with the better ability of STAT1-deficient Gr1^{int}

cells to respond to IL-6 in the context of inflammation (Figure 5h) may contribute to the increased frequency of the Gr1^{int} cells under STAT1-deficient conditions (Figure 5b).

Discussion

Previously shown to be a modulator of allergic inflammation [19], our data now demonstrate a role for an MDSC-like cell population in the lung as an innate regulator of inflammation in a model of acute bacterial pneumonia. This delicate balance required between appropriate inflammation to clear pathogens in infected tissue and the removal of associated immune-mediated pathology to minimize collateral tissue damage is well appreciated in the literature but not adequately studied [4]. We show that although early IL-10 production hampers bacterial clearance from the lung, its complete absence prevents resolution of neutrophilic inflammation and recovery of mice. In the lung, accumulation of interstitial neutrophils during non-resolving pneumonia has been associated with the hallmarks of acute lung injury [7,8,10]. However, no study to date has described which cells participate in the normal resolution of inflammation after bacterial infection so that the process can be improved when in jeopardy. We show that the host expands Gr1^{int} MDSC-like cell numbers in the tissue in response to bacterial infection with a delayed kinetics. These MDSC-like Gr1^{int} cells produce IL-10 and can efferocytose apoptotic neutrophils. Interestingly, efferocytosis by MDSC-like cells is aided by IL-10, inviting speculation regarding autocrine/paracrine enhancement of efferocytosis during the resolution phase of inflammation. We show that deletion of STAT1 lowers the neutrophilic burden in the lung with concomitant increase in the proportion of MDSC-like cells without causing undue mortality of the mice. This is important since a combination of a STAT1 inhibitor and appropriate antibiotic therapy may help address non-resolving pneumonia with decreased associated mortality.

An important initial goal in this study was to determine a dose of *K. pneumoniae* that would cause ~50% lethality early in WT mice but would be less lethal to IL-10–/– mice. This is because from the existing literature, it was clear that early IL-10 inhibits neutrophil recruitment [4,12,13], neutrophils being important in defense against this bacterium. We therefore expected that we would be able to arrive at a dose that at an early time point would impart a survival benefit to the IL-10–/– mice as compared to the WT mice. We reproducibly observed 100% survival rate in WT mice when a 100 CFU of this bacterium was used but 50% survival when a log higher dose was used. 100 CFU induced minor cellular infiltration and very minimal lung injury in all WT or IL-10–/– animals (data not shown). Thus a low dose would not have allowed us to address our main question, which was the role of IL-10 in host defense against *K. pneumoniae* late after infection, this question being pertinent in resolving versus non-resolving pneumonia. Using the 1000 CFU dose, although the IL-10–/– mice fared better initially, they were near death by 144h (6 days) and had to be sacrificed. With the dying IL-10–/– mice we also sacrificed the surviving WT mice to analyze parameters that were different between the WT and the IL-10–/– mice 144 h post infection (Fig. 1, Supp Figs S1–S3). With a lower dose of 100 CFU, there would not have been enough early immune activation to trigger continued neutrophil influx, which contributed to mortality in the IL-10–/– mice at the 144h time point. Collectively, while inclusion of data from mice that needed to be sacrificed early could have influenced the results presented, we feel that our analysis of mice that survived

up to 144h has not biased our data that has addressed differences between IL-10-sufficient and IL-10-deprived state late after infection. Since *K. pneumoniae* is an extremely virulent bacterium for many strains of mice, the LD_{50} is quite low. For reproducibility, we infected mice with 1000 CFU each time, which ensured a difference in the outcome between WT and IL-10–/– mice.

IL-10 can have opposite effects depending on context and timing. For example, during murine pneumonia induced by a lethal dose of *K. pneumoniae*, instillation of anti-IL-10 before infection improved bacterial clearance [12]. A similar observation was made when early production of anti-inflammatory mediators including IL-10 was shown to be deleterious to recruitment of neutrophils for defense against *Streptococcus pneumoniae* [35]. In each of these studies, anti-IL-10 was administered immediately before infection and lethal doses of bacteria were used. In contrast, complete absence of IL-10 has been shown to increase tissue injury in multiple infection models involving protozoa, bacteria, and nematodes [36] and also evident in our model of bacterial pneumonia in which an LD_{50} dose of *K. pneumoniae* was used. In our previous study, we showed that the expansion of the Gr1^{int} cells in response to LPS is greatly blunted in MyD88-deficient mice suggesting dependence on this adaptor protein for their accumulation [19]. Additionally, using GFP to track cells *in vivo*, we showed that a lineage negative bone marrow progenitor population when introduced intravenously into mice has the ability to differentiate into MDSC-like cells in the lung after intratracheal delivery of LPS [19]. This finding was in agreement with a report showing the ability of hematopoietic stem and progenitor cells (HSPCs) in extramedullary tissues including the lung to differentiate into CD11c+Gr1+ cells in the presence of LPS [37]. It was speculated that the purpose of LPS-induced differentiation of HSPCs into myeloid cells was to boost immune surveillance although this idea was not experimentally interrogated. Taken together, it seems likely that resident HSPCs differentiate into IL-10-producing Gr1^{int} MDSC-like cells with a delayed kinetics in response to pathogen-derived signals. The molecular regulation of IL-10 in the lung MDSC-like cells has yet to be determined. However, our use of STAT1–/– mice suggests mechanisms underlying IL-10 production by these cells. Given the increased levels of IL-6-induced pSTAT3 in the STAT1-deficient Gr1^{int} cells, and IL-6 being a key cytokine produced by these cells, a likely positive regulator of IL-10 in the Gr1^{int} cells is STAT3 [38,39]. Reciprocally, as previously observed [40,41], STAT1 may negatively regulate IL-10 in the Gr1^{int} cells since a significantly higher level of IL-10 was detected in the lungs of STAT1-deficient mice as well as higher levels of IL-10 mRNA in STAT1-deficient MDSC-like cells which may be mediated by increased levels of pSTAT3 [38,39]. We observed significantly higher levels of KC expression late after infection in the lungs of IL-10–/– mice as compared to that in WT mice. KC is a known neutrophil chemoattractant during acute pulmonary inflammation [42]. Furthermore, IL-10 is known to inhibit LPS induced KC-mRNA stability [43] suggesting that lack of IL-10 is a primary mechanism contributing to increased KC in the IL-10–/– mice which is not advantageous to the host during the resolution phase.

STAT1 is important for antibacterial host defense as was shown for clearance of *Listeria monocytogenes* from livers and spleens of infected mice [44]. STAT1 expression in MDSCs

was shown to promote Arg1 and NOS2 expression and to be important for the suppressive effects of MDSCs on T cells [45]. Our previous study also showed the importance of Arg1 and IL-10 expression in the lung MDSC-like cells for inhibition of Th2 effector function [19]. However, since to date Arg1 has not been shown to promote antibacterial defense and on the contrary increased Arg1 in macrophages compromises bacterial clearance [46], enhancement of IL-10 and decrease in Arg1 expression via inhibition of STAT1 in combination with antibiotics may be an ideal therapeutic modality for non-resolving pneumonia.

In summary, in a model of bacterial pneumonia, we reveal a requirement for IL-10 in resolution of lung inflammation. We show that Gr1^{int} MDSC-like cells within the tissue compartment are a cellular source of IL-10 and that this cell type expands late after infection and aids in efferocytosis of apoptotic neutrophils. MDSCs, including the lung Gr1^{int} cells, harbor characteristics of both macrophage/monocytes and neutrophils, and therefore it has not yet been possible to selectively deplete these cells by molecular targeting, which would be beneficial in the case of tumor-associated MDSCs. However, a desirable goal in non-resolving pneumonia being to augment rather than delete this cell type, we suggest STAT1 as a suitable target to that effect with concomitant decrease in lung neutrophil burden. Our study further emphasizes the continued need for discovery of organ and cell-specific regulation of IL-10 for the purposes of immune regulation and therapeutic intervention.

Methods

Animals and reagents

Male 6–8-week old C57BL/6 mice, and IL10−/− mice on C57BL/6 background (stock number 002251), were purchased from the Jackson Laboratory (Bar Harbor, ME). STAT1−/− mice previously generated [47] were bred at the animal facility at the University of Pittsburgh. All mice were housed under pathogen-free conditions and were used between 6 and 10 weeks of age. Within experiments, the mice were age and sex matched. All studies with mice were approved by the Animal Care and Use Committee at the University of Pittsburgh. LPS from *Escherichia coli*, strain O26:B6, was obtained from Sigma (St Louis, MO). A number of fluorochrome-conjugated monoclonal antibodies were used in cell phenotyping experiments as follows: PE-labeled anti-mouse CD11b, APC-labeled anti-mouse CD11c (clone HL3), APC-labeled anti-mouse Gr1 (clone RB6-8C5), PE-labeled anti-mouse Ly6G (clone 1A8), Alexa 647-conjugated mouse anti-STAT3 (pY705, clone 4/P-STAT3), neutralizing anti-mouse IL-6, and neutralizing anti-mouse IL-10, all of which were purchased from BD Biosciences (San Jose, CA). Alexa 488-, PE- and APC-labeled anti-mouse F4/80 were purchased from Caltag Laboratories (Carlsbad, CA).

Infection

All infections were done with *K. pneumoniae* ATCC 43816 as described previously [48]. Bacterial growth medium was seeded with a 1:100 dilution of an overnight culture of *K. pneumoniae* and the culture was incubated for 2 h to attain mid logarithmic phase. The OD$_{600}$ of the culture was determined (1 OD$_{600}$ = 5×10^8 CFU) and the inoculum was diluted accordingly. For infection, the mice were anesthetized with isoflurane and 1×10^2 or 1×10^3 CFU were delivered by intratracheal instillation [49]. The exact CFU was routinely estimated

by plating dilutions of the inoculum on tryptic soy agar plates. Lung and systemic burden of *K. pneumoniae* were determined by plating dilutions of homogenized lung tissue or blood in PBS on tryptic soy agar plates. CFU were enumerated following overnight incubation at 37°C.

Generation and isolation of MDSC-like Gr1^{int} cells from the lung

MDSC-like Gr1^{int} cells were induced in the lung and isolated essentially as previously described [19]. The staining procedures to identify CD11b^{+}Gr1^{int}F4/80^{+} cells were described previously [19].

Histology and quantitation using Metamorph

Tif images of Hematoxylin & Eosin (H&E) stained lung sections (5 μm) were scanned using a Mirax MIDI (Zeiss, Budapest, Hungary) microscope. Digital images were captured using Panoramic Viewer (Version 1.14; 3D Histech) and analyzed using Metamorph. Following color separation, the blue layer was converted to monochrome. The entire lung was selected as a region and the threshold was set to 195 for all images. Region statistics were calculated. % Threshold area was determined by dividing the threshold area by the total area of the lung (region). Threshold Area/Total Area $\times$ 100 = % Threshold Area.

Efferocytosis assay

Neutrophils (PMNs) were purified from the lungs of LPS-treated mice by FACS of the Ly6G^{hi}F4/80[−] population following CD11b purification (Miltenyi Biotec Automacs technology). PMNs were cultured overnight at 37°C under serum free condition to induce apoptosis [27]. Apoptotic PMNs were detected by Annexin V/propidium iodide (PI) staining. The PMNs were labeled with DDAO-SE (Molecular Probes). Gr1^{int} cells were purified by FACS from CD11b^{+} lung cells labeled with Alexa 488-conjugated anti-mouse F4/80 and PE-conjugated anti-mouse Gr1. Apoptotic PMNs and Alexa 488 labeled Gr1^{int} cells were incubated together (10:1 ratio) for 30 minutes at 37°C. % uptake was quantified by flow cytometry. Confocal images were captured on an Olympus Fluoview FV1000 confocal microscope using a 60x Objective (NA 1.35). Following the efferocytic assay, Gr1^{int} MDSC-like cells labeled with Alexa 488-conjugated anti-mouse F4/80 and DDAO-SE (Molecular Probes)-labeled PMNs were detected using the excitation wavelengths 488 nm and 635 nm, respectively. Z-stack projections were created from 0.75 μm optical increments spanning the thickness of the cell.

Intracellular cytokine staining

Freshly isolated PMNs, Gr1^{int} and F4/80+ cells were incubated with LPS (1μg/ml) and Brefeldin A (10 μg/ml) (Sigma) for 4 h. Cells were harvested, washed twice with PBS-2% fetal bovine serum (FBS) and then fixed in 4% paraformaldehyde solution for 15 min at room temperature. After washing the cells twice, cells were incubated in permeabilization buffer for 30 min at room temperature. Cells were then centrifuged, washed in permeabilization buffer and resuspended in APC-labeled anti-mouse IL-10 (BD Biosciences, Clone# JES5-16E3) or APC-labeled Rat IgG2b control antibody for 30 min at

room temperature. Cells were finally sequentially washed in permeabilization buffer and PBS-2% FBS and analyzed by flow cytometry.

Cytokine analysis by ELISA

Cytokine production from CD11b$^+$Gr1^{int}F4/80$^+$ cells and CD11c$^+$ alveolar macrophages was assessed by culturing the cells (1×10^6 cells/ml) overnight at 37°C in RPMI 1640 (Gibco) medium supplemented with 10% heat-inactivated FBS (Gemini), 100 U/ml of penicillin, 100 μg/ml of streptomycin sulfate (Gibco, 1 mM sodium pyruvate (Gibco) and 50 μM 2-mercaptoethanol (Sigma). All reagents used had <0.6 U/ml of LPS. Secreted cytokines were measured by multiplex cytokine assay (Bio-Rad Laboratories) or ELISA (murine Duo Set; R&D Systems), according to the manufacturers' instructions.

pSTAT3 analysis

Lung cells were isolated as previously described [19]. Intracellular staining for phsophoSTAT3 (pY705) was performed according to BD Phosflow protocol for intracellular staining. Briefly, cells were left unstimulated or stimulated with recombinant mouse IL-6 at 100 ng/mL for 15 minutes at 37°C. Cells were then fixed using Fix Buffer 1 (Cat#: 557870) for 10 minutes at 37°C, washed, and stained for CD11b and Gr1 to phenotypically identify the CD11b$^+$Gr1^{int} population. Cells were permeabilized with Perm Buffer III (Cat#: 558050) on ice for 30 minutes, washed twice, and stained with pYSTAT3 (Cat#: 557815) or isotype control (Mouse IgG2ak Cat#: 558052). Intracellular staining was performed at room temperature for 30 min.

qRT-PCR

Quantitative RT-PCR was performed as previously described [25]. Tissues or cells were treated with TRIzol (Invitrogen). RNA was isoalated with the RNeasy kit (Qiagen) and treated with RNase-free DNase (Qiagen). cDNA was synthesized and used for quantitative PCR with TaqMan Gene Expression Assays (Applied Biosystems) according to the manufacturer's instructions. The level of mRNA was normalized to *HPRT1* expression, and the results were analyzed by the $2^{-\Delta Ct}$ method. Fold expression of IL-10 in STAT1–/– Gr1^{int} cells was calculated relative to expression of IL-10 in WT Gr1^{int} cells both harvested 72 h post infection with 1000 CFU *K. pneumoniae*. Fold expression of scavenger receptors in IL-10–/– Gr1int cells was calculated relative to expression in WT Gr1int cells both harvest 72 h post infection with 1000 CFU *K. pneumoniae*. The level of expression was normalized to that of the housekeeping gene HPRT and the results were analyzed using the $2^{-\Delta Ct}$ method.

Statistical analyses

Comparisons of means± s.d. were performed using one-way analysis of variance or Student t-test using GraphPad Prism software (La Jolla, CA). Differences between the groups were considered significant if $p < 0.05$.

Supplementary Material

Refer to Web version on PubMed Central for supplementary material.

Acknowledgments

References

1. Mizgerd JP. Acute lower respiratory tract infection. The New England journal of medicine. 2008; 358:716–727. [PubMed: 18272895]

2. Morens DM, Taubenberger JK, Fauci AS. Predominant role of bacterial pneumonia as a cause of death in pandemic influenza: implications for pandemic influenza preparedness. The Journal of infectious diseases. 2008; 198:962–970. [PubMed: 18710327]

3. Barton GM. A calculated response: control of inflammation by the innate immune system. J Clin Invest. 2008; 118:413–420. [PubMed: 18246191]

4. Soehnlein O, Lindbom L. Phagocyte partnership during the onset and resolution of inflammation. Nature reviews Immunology. 2010; 10:427–439.

5. Sun K, Metzger DW. Inhibition of pulmonary antibacterial defense by interferon-gamma during recovery from influenza infection. Nat Med. 2008; 14:558–564. [PubMed: 18438414]

6. Bergeron Y, Deslauriers AM, Ouellet N, Gauthier MC, Bergeron MG. Influence of cefodizime on pulmonary inflammatory response to heat-killed Klebsiella pneumoniae in mice. Antimicrob Agents Chemother. 1999; 43:2291–2294. [PubMed: 10471581]

7. Lee WL, Downey GP. Neutrophil activation and acute lung injury. Curr Opin Crit Care. 2001; 7:1–7. [PubMed: 11373504]

8. Abraham E. Neutrophils and acute lung injury. Crit Care Med. 2003; 31:S195–199. [PubMed: 12682440]

9. Mizgerd JP. Lung infection--a public health priority. PLoS Med. 2006; 3:e76. [PubMed: 16401173]

10. Balamayooran G, Batra S, Fessler MB, Happel KI, Jeyaseelan S. Mechanisms of neutrophil accumulation in the lungs against bacteria. Am J Respir Cell Mol Biol. 2010; 43:5–16. [PubMed: 19738160]

11. Ware LB, Matthay MA. The acute respiratory distress syndrome. N Engl J Med. 2000; 342:1334–1349. [PubMed: 10793167]

12. Greenberger MJ, et al. Neutralization of IL-10 increases survival in a murine model of Klebsiella pneumonia. J Immunol. 1995; 155:722–729. [PubMed: 7608550]

13. Medeiros AI, Serezani CH, Lee SP, Peters-Golden M. Efferocytosis impairs pulmonary macrophage and lung antibacterial function via PGE2/EP2 signaling. J Exp Med. 2009; 206:61–68. [PubMed: 19124657]

14. Steinhauser ML, et al. IL-10 is a major mediator of sepsis-induced impairment in lung antibacterial host defense. J Immunol. 1999; 162:392–399. [PubMed: 9886412]

15. Capsoni F, et al. IL-10 up-regulates human monocyte phagocytosis in the presence of IL-4 and IFN-gamma. J Leukoc Biol. 1995; 58:351–358. [PubMed: 7665991]

16. Michlewska S, Dransfield I, Megson IL, Rossi AG. Macrophage phagocytosis of apoptotic neutrophils is critically regulated by the opposing actions of pro-inflammatory and anti-inflammatory agents: key role for TNF-alpha. FASEB J. 2009; 23:844–854. [PubMed: 18971259]

17. Fessler MB, et al. A role for hydroxy-methylglutaryl coenzyme a reductase in pulmonary inflammation and host defense. Am J Respir Crit Care Med. 2005; 171:606–615. [PubMed: 15591471]

18. Nick JA, et al. Role of p38 mitogen-activated protein kinase in a murine model of pulmonary inflammation. J Immunol. 2000; 164:2151–2159. [PubMed: 10657669]

19. Arora M, et al. TLR4/MyD88-induced CD11b+Gr-1 int F4/80+ non-migratory myeloid cells suppress Th2 effector function in the lung. Mucosal Immunol. 2010; 3:578–593. [PubMed: 20664577]

20. Condamine T, Gabrilovich DI. Molecular mechanisms regulating myeloid-derived suppressor cell differentiation and function. Trends in immunology. 2011; 32:19–25. [PubMed: 21067974]

21. Jeisy-Scott V, et al. Increased MDSC accumulation and Th2 biased response to influenza A virus infection in the absence of TLR7 in mice. PLoS One. 2011; 6:e25242. [PubMed: 21966467]

22. Cai S, Batra S, Shen L, Wakamatsu N, Jeyaseelan S. Both TRIF- and MyD88-dependent signaling contribute to host defense against pulmonary Klebsiella infection. J Immunol. 2009; 183:6629–6638. [PubMed: 19846873]

23. Jones RN. Microbial etiologies of hospital-acquired bacterial pneumonia and ventilator-associated bacterial pneumonia. Clin Infect Dis. 2010; 51 (Suppl 1):S81–87. [PubMed: 20597676]

24. Nefedova Y, et al. Hyperactivation of STAT3 is involved in abnormal differentiation of dendritic cells in cancer. J Immunol. 2004; 172:464–474. [PubMed: 14688356]

25. Fei M, et al. TNF-alpha from inflammatory dendritic cells (DCs) regulates lung IL-17A/IL-5 levels and neutrophilia versus eosinophilia during persistent fungal infection. Proc Natl Acad Sci U S A. 2011; 108:5360–5365. [PubMed: 21402950]

26. Han J, Brown T, Beutler B. Endotoxin-responsive sequences control cachectin/tumor necrosis factor biosynthesis at the translational level. J Exp Med. 1990; 171:465–475. [PubMed: 2303781]

27. Filardy AA, et al. Proinflammatory clearance of apoptotic neutrophils induces an IL-12(low)IL-10(high) regulatory phenotype in macrophages. J Immunol. 2010; 185:2044–2050. [PubMed: 20660352]

28. Chalmin F, et al. Membrane-associated Hsp72 from tumor-derived exosomes mediates STAT3-dependent immunosuppressive function of mouse and human myeloid-derived suppressor cells. J Clin Invest. 2010; 120:457–471. [PubMed: 20093776]

29. Qing Y, Stark GR. Alternative activation of STAT1 and STAT3 in response to interferon-gamma. J Biol Chem. 2004; 279:41679–41685. [PubMed: 15284232]

30. Hu X, Ivashkiv LB. Cross-regulation of signaling pathways by interferon-gamma: implications for immune responses and autoimmune diseases. Immunity. 2009; 31:539–550. [PubMed: 19833085]

31. Shuai K, Liu B. Regulation of JAK-STAT signalling in the immune system. Nature reviews Immunology. 2003; 3:900–911.

32. Najjar I, Fagard R. STAT1 and pathogens, not a friendly relationship. Biochimie. 2010; 92:425–444. [PubMed: 20159032]

33. Flannagan RS, Cosio G, Grinstein S. Antimicrobial mechanisms of phagocytes and bacterial evasion strategies. Nat Rev Microbiol. 2009; 7:355–366. [PubMed: 19369951]

34. Rahimi AA, Gee K, Mishra S, Lim W, Kumar A. STAT-1 mediates the stimulatory effect of IL-10 on CD14 expression in human monocytic cells. J Immunol. 2005; 174:7823–7832. [PubMed: 15944287]

35. Knapp S, et al. Alveolar macrophages have a protective antiinflammatory role during murine pneumococcal pneumonia. Am J Respir Crit Care Med. 2003; 167:171–179. [PubMed: 12406830]

36. Couper KN, Blount DG, Riley EM. IL-10: the master regulator of immunity to infection. J Immunol. 2008; 180:5771–5777. [PubMed: 18424693]

37. Massberg S, et al. Immunosurveillance by hematopoietic progenitor cells trafficking through blood, lymph, and peripheral tissues. Cell. 2007; 131:994–1008. [PubMed: 18045540]

38. Stumhofer JS, et al. Interleukins 27 and 6 induce STAT3-mediated T cell production of interleukin 10. Nat Immunol. 2007; 8:1363–1371. [PubMed: 17994025]

39. Saraiva M, O'Garra A. The regulation of IL-10 production by immune cells. Nat Rev Immunol. 2010; 10:170–181. [PubMed: 20154735]

40. Hu X, et al. IFN-gamma suppresses IL-10 production and synergizes with TLR2 by regulating GSK3 and CREB/AP-1 proteins. Immunity. 2006; 24:563–574. [PubMed: 16713974]

41. Kalliolias GD, Ivashkiv LB. IL-27 activates human monocytes via STAT1 and suppresses IL-10 production but the inflammatory functions of IL-27 are abrogated by TLRs and p38. J Immunol. 2008; 180:6325–6333. [PubMed: 18424756]

42. Huang S, Paulauskis JD, Godleski JJ, Kobzik L. Expression of macrophage inflammatory protein-2 and KC mRNA in pulmonary inflammation. The American journal of pathology. 1992; 141:981–988. [PubMed: 1415488]

43. Biswas R, et al. Regulation of chemokine mRNA stability by lipopolysaccharide and IL-10. J Immunol. 2003; 170:6202–6208. [PubMed: 12794151]

44. Varinou L, et al. Phosphorylation of the Stat1 transactivation domain is required for full-fledged IFN-gamma-dependent innate immunity. Immunity. 2003; 19:793–802. [PubMed: 14670297]

45. Kusmartsev S, Gabrilovich DI. STAT1 signaling regulates tumor-associated macrophage-mediated T cell deletion. J Immunol. 2005; 174:4880–4891. [PubMed: 15814715]

46. El Kasmi KC, et al. Toll-like receptor-induced arginase 1 in macrophages thwarts effective immunity against intracellular pathogens. Nat Immunol. 2008; 9:1399–1406. [PubMed: 18978793]

47. Durbin JE, Hackenmiller R, Simon MC, Levy DE. Targeted disruption of the mouse Stat1 gene results in compromised innate immunity to viral disease. Cell. 1996; 84:443–450. [PubMed: 8608598]

48. Ye P, et al. Interleukin-17 and lung host defense against Klebsiella pneumoniae infection. Am J Respir Cell Mol Biol. 2001; 25:335–340. [PubMed: 11588011]

49. Chan YR, et al. Lipocalin 2 is required for pulmonary host defense against Klebsiella infection. J Immunol. 2009; 182:4947–4956. [PubMed: 19342674]
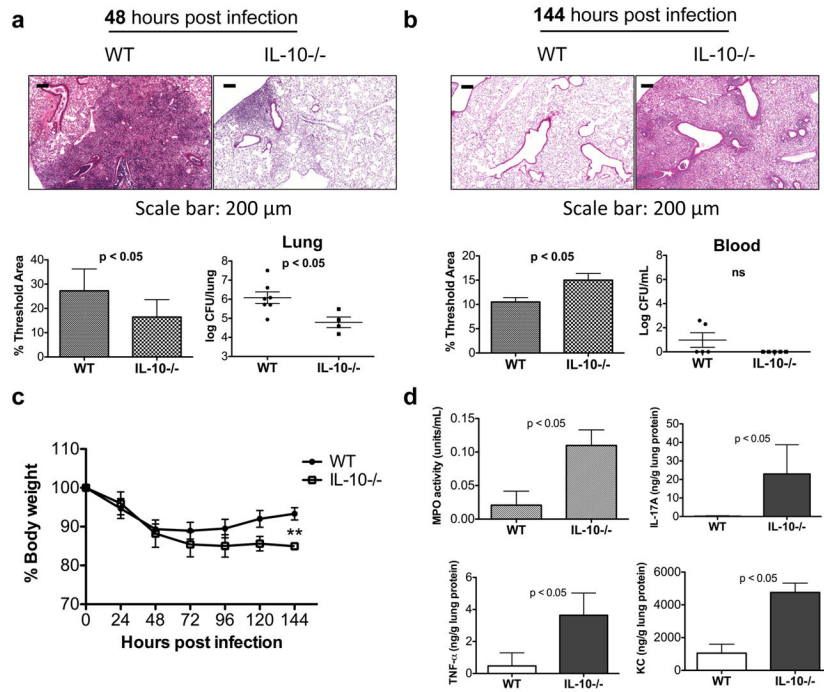
Figure 1.
IL-10 deficiency worsens outcome late after infection. To determine the role of IL-10 early versus late after infection, WT and IL-10–/– were infected with 1000 CFU of *K. pneumoniae*. (**a**) 48 h post infection mice were sacrificed. Cellular infiltration was determined by H&E staining of lung sections and inflammation in whole lung was quantified using Metamorph, as indicated by % Threshold Area. The bacterial burden in the lung was estimated by log CFU/lung. (**b**) To examine the role of IL-10 late after infection, WT and IL-10–/– mice were infected with 1000 CFU. 50% of WT mice and 20% of IL-10–/– mice were sacrificed prior to 144 h on the basis of continued weight loss, drop in body temperature and appearance (data not shown). The mice that did not show signs of morbidity were monitored until day 6 (144 h). (**b**) At 144 h post-infection, WT and IL-10–/– were examined for cellular infiltration by H&E staining and quantified by % Threshold Area. Bacterial dissemination was measured as log CFU/mL blood. (**c**) Surviving WT mice recovered from the initial weight loss unlike IL-10–/– mice. Data shown are means ± s.d. **$p < 0.01$. (**d**) MPO activity was measured in the BAL fluid 144 h post infection and total lung homogenates were analyzed for IL-17A, TNF-α, and KC levels (n=5–6 mice per group). Data shown are representative of 2 independent experiments.

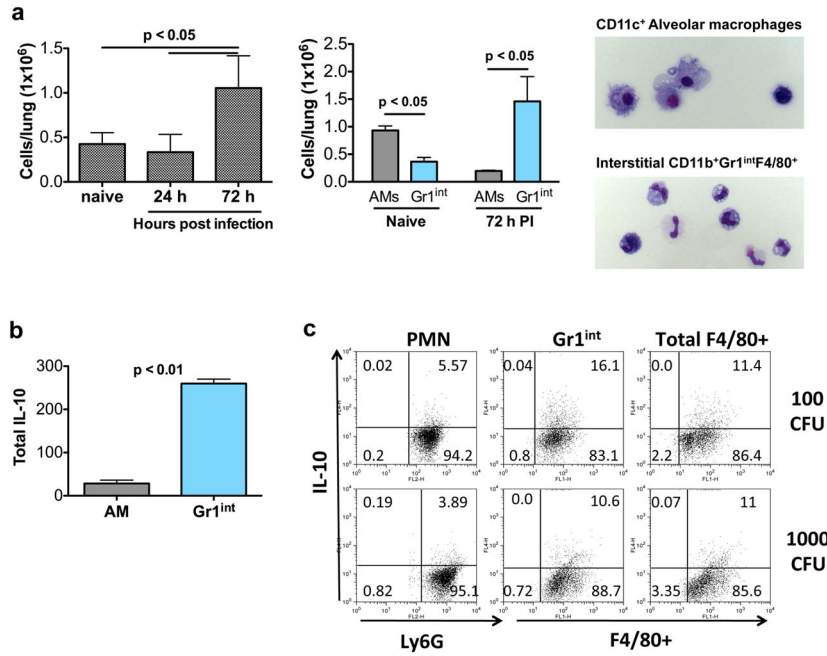**Figure 2.**
Gr1^{int} MDSC-like cells are the IL-10 producers in the lung interstitium 72 h post infection. (**a**) Gr1^{int} cell numbers were assessed at indicated times after infection of mice with 1000 CFU of *K. pneumoniae*. AMs and Gr1^{int} cells were quantified by flow cytometric analysis in naïve mice as well as in mice at 72 h post infection (PI). AMs were identified by flow cytometry based on CD11c expression and high autofluorescence while Gr1^{int} cells were CD11b+Gr1^{int}F4/80+. Morphology of each cell type is also shown. (**b**) At 72 h post infection, Gr1^{int} were purified as previously described (Arora, 2010 #148). AMs were purified by high volume lavage and CD11c magnetic purification. Cells were seeded in equal numbers and after 24 h, cell-free supernatants were analyzed by ELISA for IL-10 levels. Total IL-10 was determined by multiplying the amount of IL-10 produced per cell by the number of cells present in the lung 72 h post-infection. (**c**) Intracellular cytokine staining for IL-10 was performed on neutrophils (PMNs), Gr1^{int}, and total F4/80+ cells isolated 72 h post infection with 100 or 1000 CFU *K. pneumoniae*. CD11b+ cells were purified by AutoMACS technology. Within the CD11b+ cells, PMNs were CD11b+Ly6G^{hi}F4/80$^-$, Gr1^{int} cells were CD11b+Gr1^{int}F4/80$^+$, and total F4/80+ were CD11b+F4/80$^+$. Data shown are means ± s.d. and are representative of 2 independent experiments. For cellular quantification, mice were analyzed individually (n = 4–5 mice per group). For cell purification and sorting to determine cytokine production, cells from 3–4 mice pooled per group.
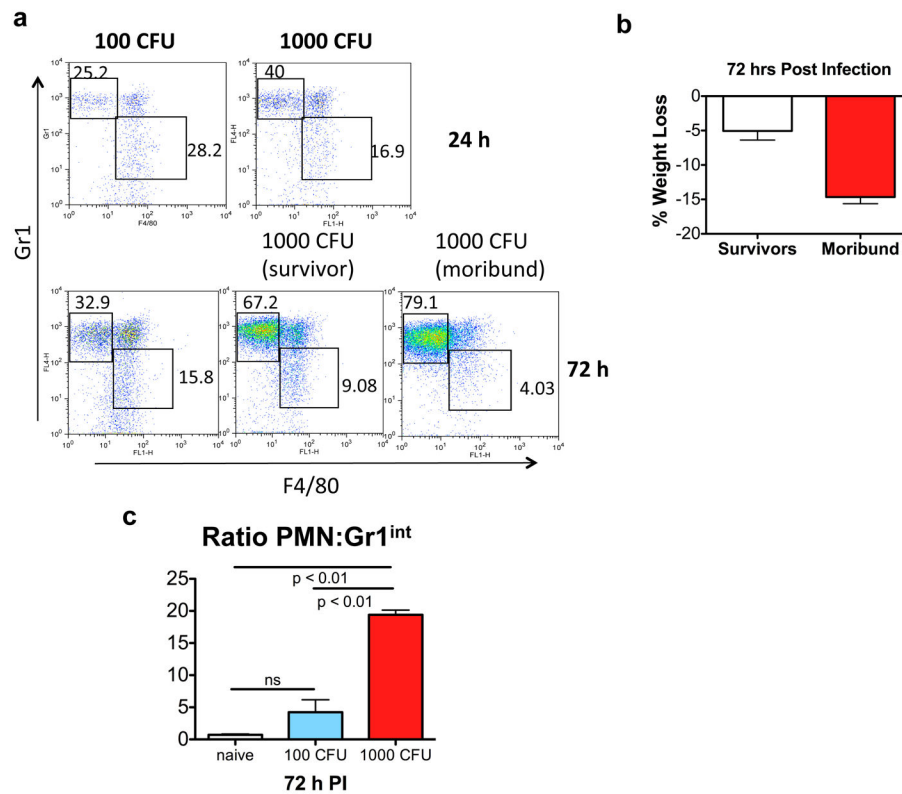
Figure 3.
Increased PMN infiltration in the lung at higher bacterial burden resulting in an increased PMN:Gr1^{int} ratio. (**a**) The CD11b$^+$ population in the lung was analyzed for Ly6G or Gr1 and F4/80 expression. Ly6G^{hi}F4/80$^-$ cells represent PMNs whereas Gr1^{int}F4/80$^+$ cells are the Gr1^{int} lung-MDSC like cells. 1000 CFU of bacteria induced more PMN infiltration than 100 CFU at both 24 and 72 h post infection. (**b**) Mice infected with 1000 CFU can be divided into 2 groups on the basis of weight loss 72 h post infection. Therefore, panel (**a**) also depicts representative flow plot of a moribund versus a surviving mouse. (**c**) A significantly higher PMN to Gr1^{int} ratio in the lung tissue with 1000 CFU as compared to 100 CFU of *K. pneumoniae*. Total cell numbers (in millions) 72 h post infection were PMN: 5.03 +/−1.54; Gr1^{int}: 1.03 +/−0.37 (with 100 CFU) and PMN:15.3 +/−4.3; Gr1^{int}: 0.94 +/−0.36 (with 1000 CFU). Data shown are means ± s.d. and are representative of 2 independent experiments. For cellular quantification and determination of ratios, mice were analyzed individually (n = 4–5 mice per group).
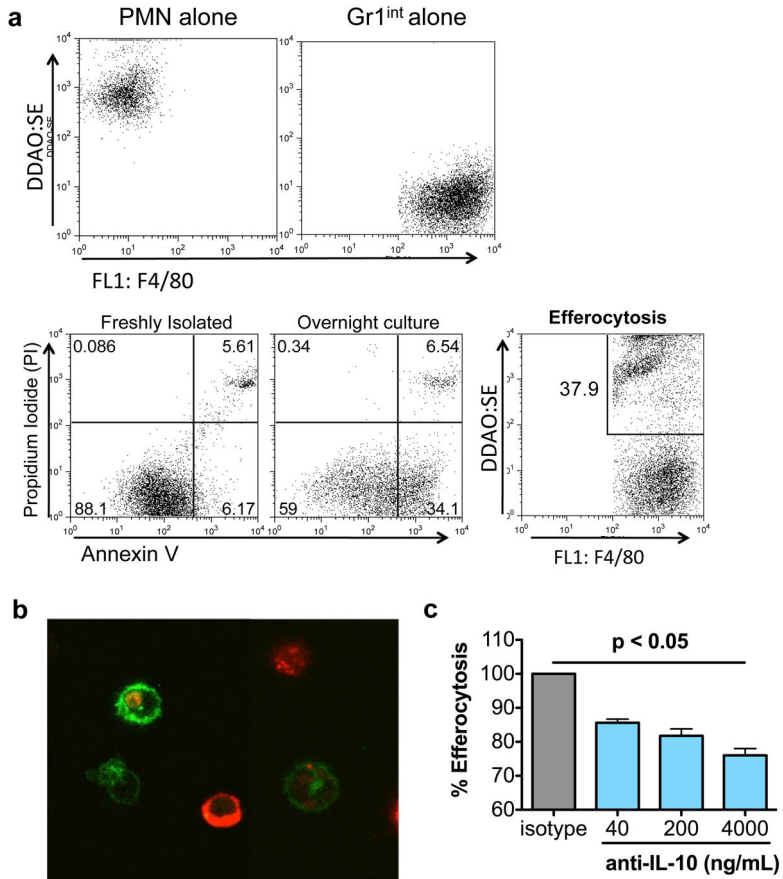
Figure 4.
Gr1^{int} cells efferocytose apoptotic PMNs. (**a**) PMNs were purified from the lungs of LPS treated mice (10 μg/day for 3 days) and plated overnight under serum free conditions (2×10^6 cells/mL) to induce apoptosis. 35% of the live PMNs (based on forward and side scatter) were annnexin V$^+$/PI$^-$. Gr1^{int} cells were purified from the lungs of LPS-treated mice as F4/80$^+$Gr1^{int} cells by FACS of Alexa-488- and PE-labeled CD11b+ cells. PMNs were labeled with DDAO-SE (Molecular Probes). Gr1^{int} and PMNs were cultured together in a 1:10 ratio for 30 min at 37°C. The cells were washed twice and percent uptake was determined by flow cytometry. (**b**) Confocal images of apoptotic PMNs (red) inside of Gr1^{int} (green) cells. Z-stack projections were taken to confirm intracellular location (not shown). (**c**) Antibody-mediated neutralization of IL-10 in culture during efferocytosis assay reduced uptake of PMNs by Gr1^{int} cells. Data shown are representative of 2 independent experiments. For cell purification and sorting of lung-MDSCs and PMNs, 3–4 mice were treated and total lung cells were pooled for subsequent purification.
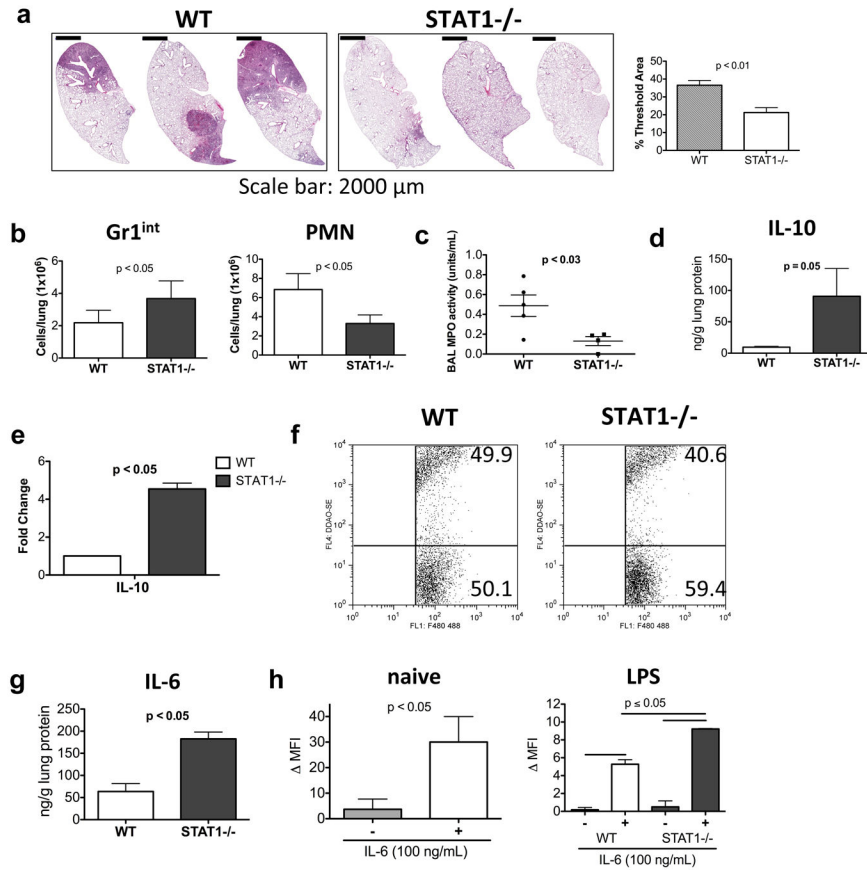
Figure 5.
STAT1−/− show reduced cellular infiltration upon gross examination with decreased frequency of PMNs and increased frequency of Gr1^{int} cells in the lungs following 1000 CFU *K. pneumoniae* infection. (**a**) WT and STAT1−/− were infected with 1000 CFU. 72 h post infection lungs were examined for histopathology by H&E staining and the stained lung sections were quantified using Metamorph. (**b**) The numbers of Gr1^{int} cells increases and PMNs decrease in STAT1−/− as compared to WT 72 h post infection with 1000 CFU of *K. pneumoniae*. (**c**) STAT1−/− mice showed reduced MPO activity in the BAL fluid compared to that observed in WT mice. (**d**) Lung IL-10 levels were increased in STAT1−/− mice as compared to that in WT mice. (**e**) Increased IL-10 mRNA levels in STAT1-deficient Gr1^{int} cells as determined by qRT-PCR analysis (n=3–4 mice/group). (**f**) STAT1−/− Gr1$^{int cells}$ can efferocytose apoptotic PMNs similar to WT Gr1^{int} cells. (**g**) Lung IL-6 levels were increased in STAT1−/− mice as compared to that in WT mice. (**h**) The level of Gr1^{int} pSTAT3 expression was analyzed in naïve mice or mice treated with LPS (10 μg/day for 3 days). Analysis of pSTAT3 levels in WT and STAT-1-deficient MDSC-like cells ± IL-6 (100 ng/ml) reveals that pSTAT3 level is increased in STAT1−/− Gr1^{int} compared to WT. The level of pSTAT3 expression expressed as   MFI represents the difference in mean channel fluorescence intensity of positive staining cells and of those stained with isotype controls. Data shown are means ± s.d. (n=3 mice/group) and are representative of two independent experiments.